Theoretical and experimental approaches to determine the mass transfer coefficient in the steel/slag/refractory system

M Schickbichler[1], E Karimi-Sibaki[2], A Kharicha[3] and S K Michelic[4]

1. PhD student, Christian Doppler Laboratory for Inclusion Metallurgy in Advanced Steelmaking, Leoben Styria 8700.
   Chair of Ferrous Metallurgy, Leoben Styria 8700.
   Email: Manuel.Schickbichler@unileoben.ac.at
2. Privatdozent, Christian Doppler Laboratory for Metallurgical Applications of Magnetohydrodynamics, Leoben Styria 8700.
   Chair of Simulation and Modeling Metallurgical Processes, Leoben Styria 8700.
   Email: Ebrahim.Karimi-Sibaki@unileoben.ac.at
3. Full professor, Christian Doppler Laboratory for Metallurgical Applications of Magnetohydrodynamics, Leoben Styria 8700.
   Chair of Simulation and Modeling Metallurgical Processes, Leoben Styria 8700.
   Email: Abdellah.Kharicha@unileoben.ac.at
4. Full professor, Christian Doppler Laboratory for Inclusion Metallurgy in Advanced Steelmaking, Leoben Styria 8700.
   Chair of Ferrous Metallurgy, Leoben Styria 8700.
   Email: Susanne.Michelic@unileoben.ac.at

Keywords: mass transfer coefficient, steel/slag/refractory system, CFD simulation

ABSTRACT

The requirements for the controllability of metallurgical processes are increasingly becoming the focus of both industry and research. Advances in this field of research not only impact the stability of processes but often also influence the quality of the final product. One important way to examine processes in depth, and thus show potential for improvement, is to describe them using physics-driven models. In metallurgy, thermodynamic and kinetic descriptions of interactions between individual components of a system are often used to describe and analyse important metallurgical phenomena across the entire process. However, for the creation of physics-based models, boundary conditions and process variables must be implemented to enable a description that is as realistic as possible. The collection and generalization of boundary conditions and process variables is, therefore, an important step towards functional models.

The focus of this study is the determination of mass transfer coefficients between all components in a steel/slag/refractory system. For this purpose, experimental and theoretical methods are applied. Laboratory scale experiments are carried out in an induction furnace, and the mass transfer coefficients of the defined steel/slag/refractory system are calculated from changes in the chemical composition of the various components. Additionally, a calculation of the mass transfer coefficients based on dimensionless quantities is carried out. By comparing the values of the mass transfer coefficients determined theoretically and those determined experimentally in the trials, the suitability of the calculation is examined. The collection of mass transfer coefficients provides essential findings for future kinetic descriptions of inclusion modification based on the effective equilibrium reaction zone (EERZ) approach.

INTRODUCTION

The modelling of metallurgical processes is becoming increasingly important due to the ever-increasing demands on materials and process control. Two different approaches for developing models have become the main focus of current research. Data-driven models, such as those described by Boto *et al* (2022), are based on the computer-aided processing and analysis of historical data in order to establish relationships between process inputs and process outputs. In contrast, in physics-based models, as shown in the work of Scheller and Shu (2014), relationships between process inputs and process outputs are defined by physical laws. As Johansen *et al* (2023) have described, the advantage of physics-based models, despite the required in-depth knowledge of the process itself, is that no large amounts of historical data are required to develop the model, as is the case with the data-driven model. Kouraytem *et al* (2021) note that physics-based models are, therefore, more suitable, especially for production processes with many different end products.

One way of describing metallurgical processes, such as the modification of inclusions or the interaction of phases using physics-based models, is with the effective equilibrium reaction zone (EERZ) model developed by Hsieh *et al* (1983). Ding *et al* (2000) describe this as a thermodynamic and kinetic model of the interaction between individual system components based on the consideration that a local thermodynamic equilibrium is reached at the interfaces of these system components. Using the EERZ model, several researchers (van Ende *et al*, 2011; You, Michelic and Bernhard, 2020; Goulart, Castro and Costa e Silva, 2023) have already investigated the processes in various metallurgical aggregates.

To describe the kinetics in the EERZ model, the mass transfer coefficients of the individual system components must be determined. One way to achieve this in the steel/slag/refractory system is to use the method described by Shin, Chung and Park (2017) to empirically determine these coefficients based on the change in the composition of the individual systems over time. Another method for determining mass transfer coefficients is to calculate them from dimensionless parameters of the respective interfaces, as described by Zhang and Xu (2003). Since complex flow conditions are often found in metallurgical processes, the method of computational fluid dynamics (CFD) is often used to determine the dimensionless coefficients, as in the work of Vollmann and Harmuth (2010).

To simulate the processes in the experimental system (induction furnace) used in this work, the interactions between the liquid phases and electromagnetic fields must be considered. This field of research, known as magnetohydrodynamics (MHD), has already been explored in detail by other researchers (eg. Al-Nasser *et al,* 2021; Kharicha *et al*, 2021; Zhang *et al*, 2022). Furthermore, Perminov and Nikulin (2016) specifically investigated flow conditions in induction furnac including MHD.

The present work focuses on the determination of mass transfer coefficients at laboratory scale, using the methods described in the same system. The associated comparison of the procedures is intended to demonstrate their equivalence. The aim is to enable a target-oriented selection of a determination method for mass transfer coefficients, even for processes for which one of the methods is not applicable. For future process descriptions based on the EERZ model, this represents a possibility for standardizing the model creation in the future.

MATERIALS AND METHODS

To investigate the kinetic parameters in the present work, laboratory experiments were carried out in an Inductotherm 150-kg A/F-type induction furnace. An isostatically pressed magnesium/aluminium spinel crucible with low values of silicon was used as a melting vessel. The respective charge materials (steel and steel/slag) were placed in the furnace for the test and inductively heated to a predetermined temperature. The temperature was controlled by adjusting the power applied and regularly measuring the temperature using immersion thermocouples. To prevent possible reactions between liquid phases and the atmosphere, the bath surface was flushed with argon throughout the experiment. The described test setup is shown schematically in Figure 1. The setup features a crucible with a diameter of 14 cm and a height of 27 cm. Additionally, the steel pool has a height of 10 cm, and the slag layer is 3 cm thick.

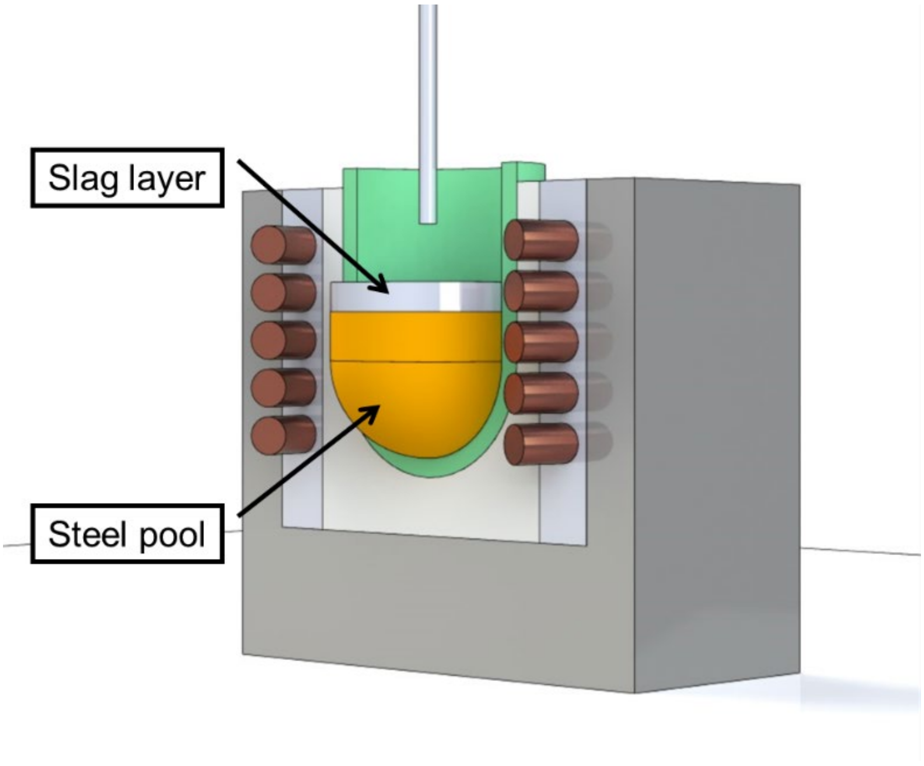

Figure 1. Schematic representation of the experimental setup.

The reactions of different phases and the associated changes in their compositions are described in this paper using the EERZ model. In considering the metallurgical processes, reaction zones are identified between all relevant phases. According to the model, a local thermodynamic equilibrium is established in the reaction zones at the interfaces of two phases in a defined time step. The quantities of phases that react with each other in the reaction zones are taken from a bulk zone that is not involved in the reaction at each reaction step. After the time step, in which a thermodynamic equilibrium is reached between the phases and the quantities of phases involved in the reaction zones change in their composition, these are reintegrated into the bulk zone of the respective phase and, thus, change the chemical composition of this for the next time step. The procedure described above makes it possible to investigate processes thermodynamically and kinetically, which in turn enables us to predict changes in concentration during the process. The sample crucible used, with the phases involved, the respective bulk zones and the reaction zones identified as relevant for this work, are shown schematically in Figure 2.

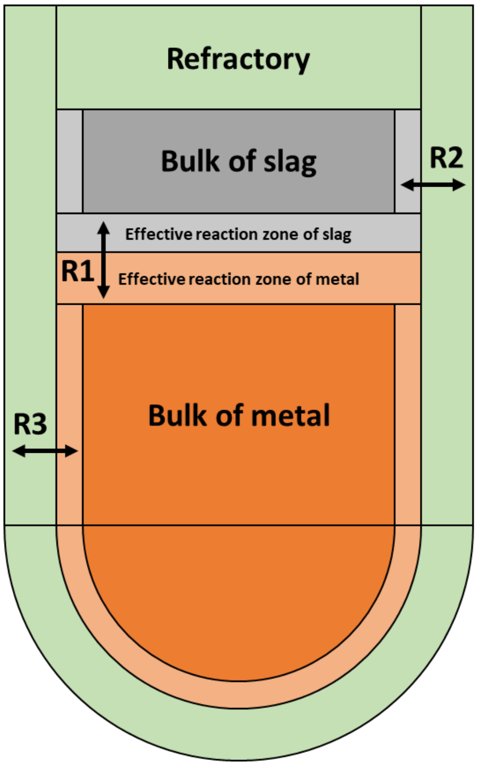

Figure 2. Schematic representation of the reaction zones in the experimental setup.

The following reactions between the two phases are examined within this work:

- R1: Reaction between liquid steel and slag
- R2: Reaction between liquid slag and refractory material
- R3: Reaction between liquid steel and refractory material

Two different experiments were conducted in the induction furnace to investigate the described reactions. The specifications of those experiments are summarised in Table 1.

Table 1. Specifications of the conducted experiments.

Trial	Temperature [°C]	Phases involved	Investigated reactions	Determined concentration curves
T1	1500	Steel (10 kg), refractory material	R3	Mg content
T2	1500	Steel (10 kg), Slag (2 kg), Refractory material	R1	Cr content
			R2	Mg content

High-speed steel was used for the tests. The chemical composition of the selected material with the DIN/EN designation HS6-5-3C is listed in Table 2.

Table 2. Chemical composition of the steel used in experiments T1 and T2.

C [wt%]	**Si [wt%]**	**Mn [wt%]**	**Cr [wt%]**	**Mo [wt%]**	**V [wt%]**	**W [wt%]**	**S [wt%]**	**O [wt%]**	**Fe [wt%]**
1.29	0.60	0.30	4.20	5.00	3.00	6.30	0.012	0.004	balance

The slag composition used in the tests is shown in Table 3. The slag for these tests was selected to present as a liquid phase at a planned test temperature of 1500°C. By performing a thermodynamic calculation using FactSage, the liquidus temperature of the slag was calculated to be 1404°C.

Table 3. Chemical composition of the slag used in experiment T2.

MgO [wt%]	**SiO_2 [wt%]**	**CaO [wt%]**
25	55	20

The tests aimed to produce concentration profiles of the different compounds over time. In order to determine these in defined time steps, steel samples were taken using unkilled lollipop samplers and slag samples via immersion sampling. The first sampling, performed shortly after the phases had completely melted, also marked the starting point of the subsequent analysis. The steel and slag samples were analysed using spark spectroscopy (SPECTROMAXx) and X-ray fluorescence analysis (ARL Fisons Instruments 8410), respectively.

Concept of calculation

To describe the phase reactions using the EERZ model, it is necessary to obtain the mass transfer coefficients (k_i) as determining kinetic parameters. So the zone thicknesses of the corresponding effective reaction zone can be calculated.

As shown by Shin, Chung and Park (2017), the mass transfer coefficients of the phases can be derived from the concentration curves of the bulk zones over time. The relations proposed by Jönsson and Jonsson (2001) for increasing and decreasing concentration curves, respectively, can be used for this purpose:

$$\frac{dMe_{BZ}[wt\%]}{dt} = k_i * \frac{\rho_i * A}{W_i} * (Me_{RZ}[wt\%] - Me_{BZ}[wt\%]) \quad [1]$$

$$\frac{dMe_{BZ}[wt\%]}{dt} = k_i * \frac{\rho_i * A}{W_i} * (Me_{BZ}[wt\%] - Me_{RZ}[wt\%]) \quad [2]$$

The values Me_{BZ} and Me_{RZ} represent the concentrations of the analysed metals in the bulk zone and the reaction zone, respectively. Furthermore, the variables ρ_i, W_i and A are the density, the total mass of the investigated phase and the contact surface on which the reaction takes place, respectively. Shin, Chung and Park (2017) showed that by including considerations of the equilibrium distributions of the investigated metals in the phases, a conversion of Eq.[1] and Eq.[2] is possible as follows:

$$-\left(\frac{Me_{eq}[wt\%]}{Me_0[wt\%]}\right) * \frac{W_i}{\rho_i * A} * \ln\left(\frac{Me_{BZ}[wt\%] - Me_{eq}[wt\%]}{Me_0[wt\%] - Me_{eq}[wt\%]}\right) = k_i * t \quad [3]$$

$$-\left(\frac{Me_0[wt\%] - Me_{eq}[wt\%]}{Me_0[wt\%]}\right) * \frac{W_i}{\rho_i * A} * \ln\left(\frac{Me_{BZ}[wt\%] - Me_{eq}[wt\%]}{Me_0[wt\%] - Me_{eq}[wt\%]}\right) = k_i * t \quad [4]$$

Here, the values Me_0 and Me_{eq} represent the concentration of the metal in the phase at time t=0 and the concentration of the metal in thermodynamic equilibrium, respectively.

By plotting the left part of Eq.[3] or Eq.[4] on the ordinate and the time on the abscissa of a diagram, the corresponding mass transfer coefficient can be obtained from the slope of a regression line placed on the curve. The values Me_{BZ} for the respective times and Me_0 are determined from the concentration curves resulting from the induction furnace experiments. The values for W_i, ρ_i and A are defined by the specifications of the respective test (shown in Table 1). To obtain Me_{eq}, thermodynamic calculations were also carried out using FactSage for the respective systems.

Concept of simulation

A CFD simulation of the system, shown in Figure 1, was conducted as a further method of determining the effective mass transfer coefficients. Considering the symmetrical aspects of geometry, a 2D axisymmetric computational domain is assumed for the calculation. Also, it is considered that slag and steel are isothermal, with the temperature specified in the system. The analysis involves solving the electromagnetic and flow fields in the molten slag and steel under the assumption that the interface between slag and steel remains stationary. The finite volume method (FVM) is employed for solving the governing equations of the flow and magnetic field. These equations, along with the boundary conditions, are implemented in ANSYS Fluent v.15.0 using user-defined functions (UDF), as referenced in the work of Karimi-Sibaki *et al* (2018). The calculated time-averaged Lorentz force is incorporated as a source term in the momentum equation, following guidelines described by Karimi-Sibaki *et al* (2018). Since the system is considered isothermal, thermal buoyancy effects are neglected, leading to flow driven solely by the Lorentz force. This results in the generation of the well-known electro-vortex flow within the slag and steel.

The outcomes of the simulation yielded the velocity field within the distinct phases involved. Also, simulation results provided the distribution of velocity magnitude along the interfaces. To compute the mass transfer coefficients at these interfaces, it is necessary to calculate the mean Reynolds number (Re) and the mean Schmidt number (Sc) as follows:

$$Re = \frac{\bar{u} * L}{\nu} \qquad [5]$$

$$Sc = \frac{\nu}{D} \qquad [6]$$

The variables $\bar{u}$, L, ν and D are the mean values of the characteristic velocity over the length of the respective interface, the characteristic length, the kinematic viscosity, and the diffusion coefficient of the investigated species, respectively.

The Sherwood number (Sh) can subsequently be calculated from the resulting values for Re and Sc for each of the interfaces between phases as a further dimensionless parameter. For this purpose, the empirical relationship developed by Vollmann and Harmuth (2010) for rotational disks is applied.

$$Sh = 1.468 * Re^{0.526} * Sc^{0.199} \qquad [7]$$

Finally, the described relationship (Eq.[7]) can be equated with the generally valid definition of Sh which is shown in Eq.[8], and the mass transfer coefficient at the respective interface can be calculated. In this context, Sh is generally formulated as follows:

$$Sh = \frac{k_i * L}{D} \qquad [8]$$

RESULTS

The course of the Mg content in the steel over time for test T1 is shown together with the evaluation of the measuring points according to Eq.[2] in Figure 3. Only the interaction between liquid steel and refractory material was investigated in this experiment. The slope of the regression line in Figure 3 indicates that the mass transfer of the steel at the interface of the system d has a value of $k_{st\text{-}ref} = 6 \times 10^{-7}$ m/s.

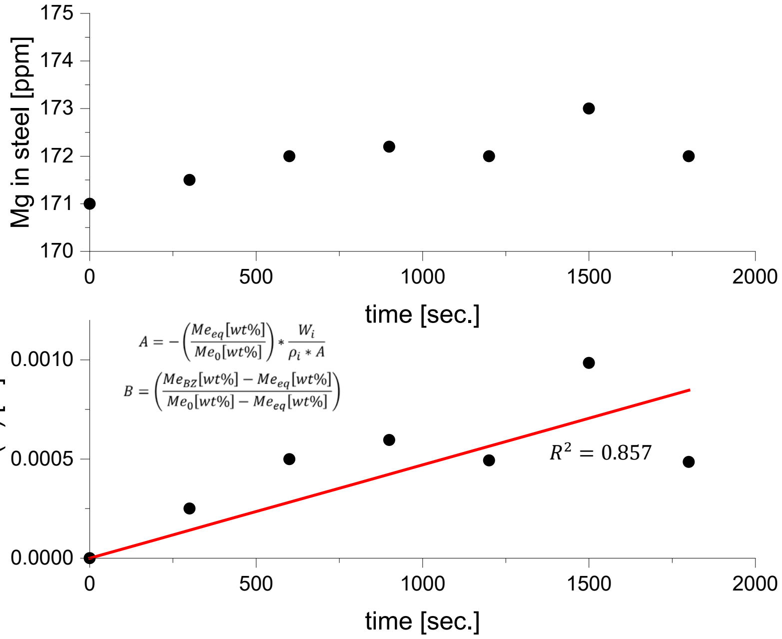

Figure 3. Development of the Mg content in steel over time in experiment T1, together with the corresponding evaluation.

In experiment T2, the slag phase was included in addition to the steel phase, as described in Table 2. The interaction between liquid slag and refractory material described in Figure 2 was investigated via the Mg content curve in the slag (see Figure 4). In the setup of test T2, in addition to the interaction investigated, Mg intake in the slag can also occur due to interaction between steel and refractory material and subsequent interaction between steel and slag. In experiment T1, however, it could be shown that the Mg uptake into the steel phase already assumes such a low value (see Figure 3) that it is acceptable to attribute the increase in the Mg content in the slag to the interaction between slag and refractory material. With this consideration, the slope of the regression line shown in Figure 4 of the measurement point evaluation according to Eq.[2] results in a mass transfer coefficient of the slag at the corresponding interface of $k_{sl\text{-}ref} = 1 \times 10^{-5}$ m/s.

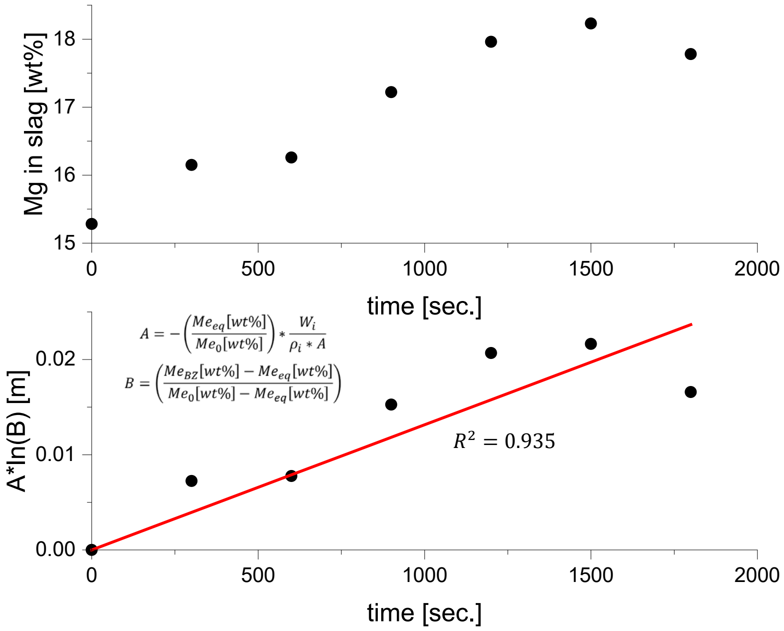

Figure 4. Development of the Mg content in slag over time in experiment T2, together with the corresponding evaluation.

In order to investigate the interaction between liquid steel and slag, the mass transfer coefficients of both the steel and the slag in the described reaction zone were determined in experiment T2. For this purpose, the course of the Cr content in both phases was investigated. The Cr curve in the steel phase is plotted in Figure 5. Since this curve shows a negative trend, the measuring points in Figure 5 were evaluated according to Eq.[4]. The slope of the regression line introduced in Figure 5 shows that the steel at the interface between steel and slag has a mass transfer coefficient of $k_{st\text{-}sl} = 2 \times 10^{-5}$ m/s.

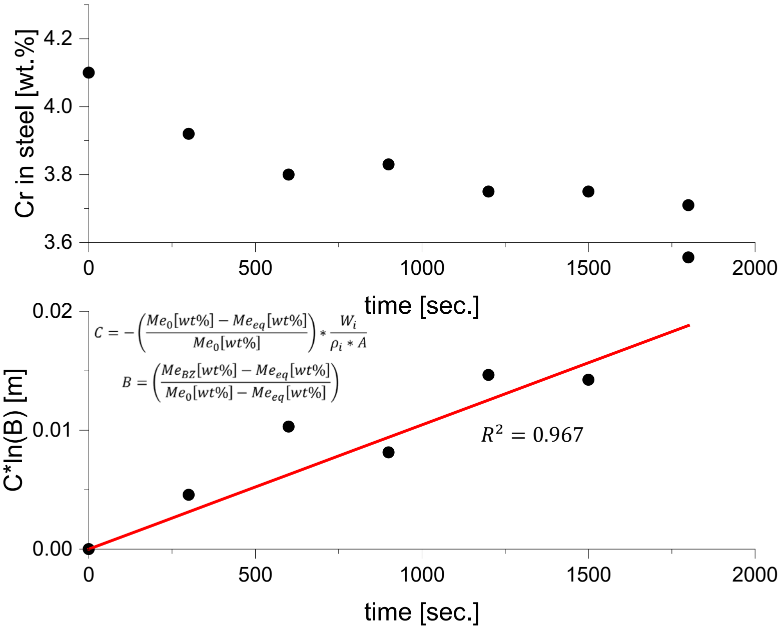

Figure 5. Development of the Cr content in steel over time in experiment T2, together with the corresponding evaluation.

To determine the mass transfer coefficient of the slag at the steel/slag interface, the Cr curve in the slag, shown in Figure 6, was analysed. For this purpose, the measuring points were also evaluated according to Eq.[3], and these are shown in Figure 6. The slope of the introduced regression curve shows that the mass transfer coefficient of the slag in this system holds a value of $k_{sl\text{-}st} = 5 \times 10^{-6}$ m/s.

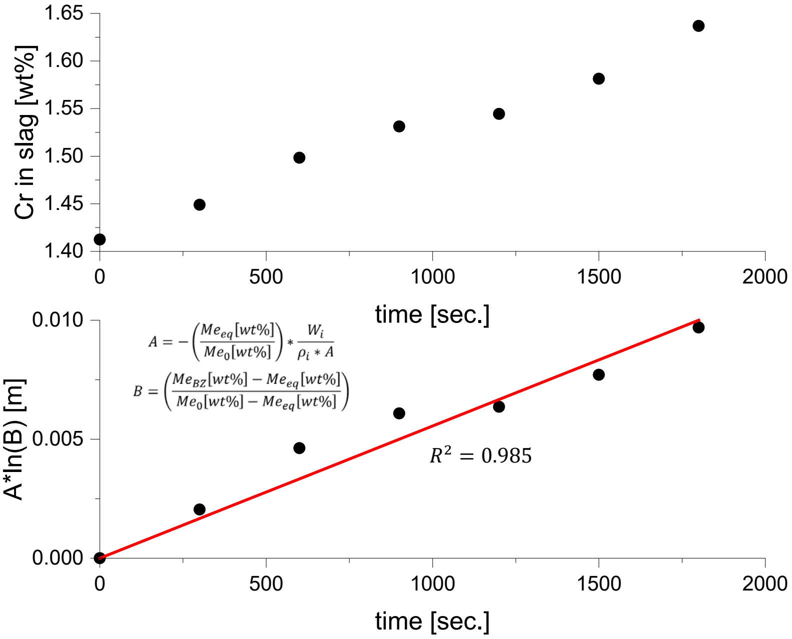

Figure 6. Development of the Cr content in steel over time in experiment T2, together with the corresponding evaluation.

Figure 7 displays the results from the CFD simulation of the induction furnace, focusing on the velocity field in the slag and steel phases. The simulation reveals distinct flow characteristics in the phase domains, including the formation of vortices in both the slag and steel phases. Also, the computed velocity distributions at the interfaces, capturing the specific flow characteristics at the phase boundaries, are the necessary data for additional calculations to determine the mass transfer coefficients.

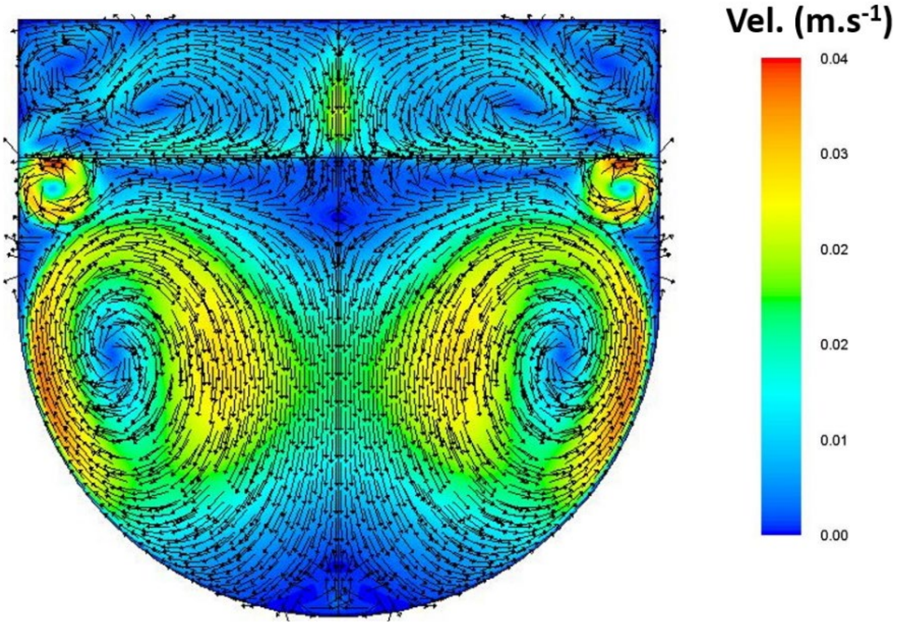

Figure 7. Velocity field obtained from CFD simulation.

To calculate the mass transfer coefficients from the velocity profiles obtained along the phase interfaces, the previously described method of calculation using the dimensionless numbers was applied for each phase. The diffusion coefficients required for the calculation were taken from the literature for similar systems and are summarised in Table 4.

Table 4. Diffusion coefficients used for the calculation of the mass transfer coefficients (based on the simulation).

System	Diffusion coefficient [m^2/s]	Source
MgO in steel	$2.7*10^{-10}$	(Lei and He, 2012)
MgO in slag	$1*10^{-8}$	(Amini *et al*, 2006)
Cr in steel	$3.04*10^{-9}$	(Ono *et al*, 1975)
Cr in slag	$4.16*10^{-10}$	(Park, Song and Min, 2004)

The kinematic viscosity of the steel required for the calculation was determined by measurements using high-temperature viscometry. Meanwhile, the kinematic viscosity of the slag was estimated with FactSage Viscosity 8.3 using the Melts database.

The mass transfer coefficients for the different interfaces calculated in the described manner are summarised in Table 5.

Table 5. Results of the calculation of the mass transfer coefficients based on the simulation.

Phase interface	Simulated mass transfer coefficients [m/s]
Steel/Refractory	$1.7*10^{-6}$
Slag/Refractory	$8.5*10^{-6}$
Steel/Slag	$2.2*10^{-5}$
Slag/Steel	$1.6*10^{-6}$

DISCUSSION

To compare both methods for determining the mass transfer coefficients at the respective interfaces, the resulting values for each method are listed in Table 6. The values of both methods are in the same order of magnitude but show a different degree of deviation in each case.

Table 6. Comparison of the values obtained for the mass transfer coefficients.

Phase interface	Mass transfer coefficients (experiments) [m/s]	Mass transfer coefficients (simulation) [m/s]
Steel/Refractory	$6.6*10^{-7}$	$1.7*10^{-6}$
Slag/Refractory	$1.1*10^{-5}$	$8.5*10^{-6}$
Steel/Slag	$1.4*10^{-5}$	$2.2*10^{-5}$
Slag/Steel	$5.2*10^{-6}$	$1.6*10^{-6}$

The deviations between the experimental method and the simulation can be explained by the assumptions made in the simulation itself and in the subsequent calculation based on it. At those phase interfaces where steel is the observed phase (Steel/Refractory and Steel/Slag) there is an overestimation of the simulation results compared to the experimentally determined values for the mass transfer coefficients. In contrast, an underestimation can be seen at those phase interfaces where slag is the observed phase (Slag/Refractory and Slag/Steel). Those findings could be connected to the fact that the kinematic viscositys of steel and slag were determined in different ways. A more realistic representation and an alignment of the experimental and simulation results may be possible if the electrical and rheological parameters of the slag were determined by actual measurements and not, as is the case in this work, based on empirical values. The estimates of the diffusion coefficients obtained from the literature should also be mentioned as a possible source of error, as they are partly based on systems that slightly differ from the actual test setup.

With regard to the usability of the collected mass transfer coefficients in the described physics-based models for determining the metallurgical processes during the test, initial calculations already show promising results. Both the mass transfer coefficients determined experimentally, and those calculated on the basis of the simulation were used to analyse the process using the EERZ model. The results, thus, obtained show good agreement with the compositional curves of steel and slag experimentally determined over the process duration. The details of the modelling will be referred to in future work.

CONCLUSIONS

Due to the increasing demands on steel materials in terms of sustainability, applicability in increasingly critical areas of use and challenging economic conditions, the controllability of manufacturing processes is increasingly becoming the focus of both research and industry. The physics-based modelling of individual processes and process chains presents an opportunity to solve the challenges mentioned in a targeted manner. In the field of metallurgy, thermodynamic and kinetic modelling, which are based on the EERZ model, are widely used. This type of model makes it possible to understand metallurgical phenomena during the production cycle over time and, thus, gain in-depth knowledge about the processes themselves. The focus of the present work is to determine the mass transfer coefficients, an important kinetic parameter for the modelling of processes using EERZ models, using different methods and, thus, comparing the suitability of the methods. For this purpose, experiments were performed under controlled conditions and a simulation was conducted, with subsequent calculations of those tests including the conditions.

The values for the mass transfer coefficients at the respective interfaces obtained using the two methods show that both approaches lead to applicable results. This can be concluded based on the respective results having the same order of magnitude and the characteristics corresponding well with the results from the literature for similar systems. Furthermore, the first experimental use of the results based on the different methods in EERZ models of the experiment shows, in both cases, a good agreement with the experimentally determined concentration curves of the phases over time.

While the values for the mass transfer coefficients at the respective interfaces determined using different methods agree well with each other and with the literature for similar systems, it is important to determine the sources for the deviations that can be found between the experimental method and the simulation. These deviations may primarily result from the assumptions made in the simulation and the subsequent calculations. The use of empirical estimates instead of actual measurements, especially when determining the parameters of the slag, leads to potential inaccuracies. The next step would be to measure these parameters specifically for the test systems and models used. This, and a repeated verification of the mass transfer coefficients obtained by means of experiments, will be the subject of further research.

ACKNOWLEDGEMENTS

The financial support by the Austrian Federal Ministry for Labour and Economy, the National Foundation for Research, Technology and Development, and the Christian Doppler Research Association is gratefully acknowledged.

REFERENCES

Al-Nasser, M, Kharicha, A, Barati, H, Pichler, C, Hackl, G, Gruber, M, Ishmurzin, A, Redl, C, Wu, M and Ludwig, A, 2021. Toward a simplified arc impingement model in a direct-current electric arc furnace, *Metals*, 11(9): 1482.

Amini, S, Brungs, M, Jahanshahi, S and Ostrovski, O, 2006. Effects of additives and temperature on the dissolution rate and diffusivity of MgO in CaO–Al2O3 slags under forced convection, *ISIJ International*, 46(11): 1554–1559.

Boto, F, Murua, M, Gutierrez, T, Casado, S, Carrillo, A and Arteaga, A, 2022. Data driven performance prediction in steel making, *Metals*, 12(2): 172.

Ding, R, Blanpain, B, Jones, P T and Wollants, P, 2000. Modeling of the vacuum oxygen decarburization refining process, *Metallurgical and Materials Transactions B*, 31(1): 197–206.

Goulart, L L d O, Castro, J A de and Costa e Silva, A, 2023. Development of a computational thermodynamics EERZ model for the improvement of hot rolled light steel profiles steel refining, *Calphad*, 81: 102550.

Hsieh, Y, Watanabe, Y, Asai, S and Muchi, I, 1983. Effect of recirculating flow rate of molten steel in refining processes, *Tetsu-to-Hagane*, 69(6): 596–603.

Johansen, S T, Løvfall, B T, Duran, T R and Zoric, J, no date. Pragmatism in industrial modelling, applied to "ladle lifetime in the steel industry", *Prepared for JSAIMM special edition on Computational Modelling*. Available from: https://arxiv.org/pdf/2302.14650.pdf.

Jönsson, P G and Jonsson, L T I, 2001. The use of fundamental process models in studying ladle refining operations, *ISIJ International*, 41(11): 1289–1302.

Karimi-Sibaki, E, Kharicha, A, Wu, M, Ludwig, A, Bohacek, J, Holzgruber, H, Ofner, B, Scheriau, A and Kubin, M, 2018. A multiphysics model of the electroslag rapid remelting (ESRR) process, *Applied Thermal Engineering*, 130: 1062–1069.

Kharicha, A, Karimi-Sibaki, E, Vakhrushev, A, Wu, M, Ludwig, A and Bohacek, J, 2021. Hydrodynamically enhanced electrochemical mass transfer on the surface of an electrically conductive droplet, *Heat and Mass Transfer*, 57(10): 1697–1705.

Kouraytem, N, Li, X, Tan, W, Kappes, B and Spear, A D, 2021. Modeling process–structure–property relationships in metal additive manufacturing: a review on physics-driven versus data-driven approaches, *Journal of Physics: Materials*, 4(3): 32002.

Lei, H and He, J, 2012. Nucleation and growth kinetics of MgO in molten steel, *Journal of Materials Science & Technology*, 28(7): 642–646.

Ono, Y and Matsumoto, S, 1975. Diffusion of chromium, manganese, and nickel in molten iron, *Transactions of the Japan Institute of Metals*, 16(7): 415–422.

Park, J H, Song, H S and Min, D J, 2004. Reduction behavior of EAF slags containing Cr2O3 using aluminum at 1793 K, *ISIJ International*, 44(5): 790–794.

Perminov, A V and Nikulin, I L, 2016. Mathematical model of the processes of heat and mass transfer and diffusion of the magnetic field in an induction furnace, *Journal of Engineering Physics and Thermophysics*, 89(2): 397–409.

Scheller, P R and Shu, Q, 2014. Inclusion development in steel during ladle metallurgical treatment - a process simulation model – part: industrial validation, *Steel Research International*, 85(8): 1310–1316.

Shin, J H, Chung, Y and Park, J H, 2017. Refractory–slag–metal–inclusion multiphase reactions modeling using computational thermodynamics: kinetic model for prediction of inclusion evolution in molten steel, *Metallurgical and Materials Transactions B*, 48(1): 46–59.

van Ende, M-A, Kim, Y-M, Cho, M-K, Choi, J and Jung, I-H, 2011. A kinetic model for the Ruhrstahl Heraeus (RH) degassing process, *Metallurgical and Materials Transactions B*, 42(3): 477–489.

Vollmann, S and Harmuth, H, 2010. Investigation of refractory corrosion of a gas-stirred steel ladle by simulation, *12th INTERNATIONAL CERAMICS CONGRESS PART I*, Advances in Science and Technology, Refractories: Recent Developments in Materials, Production and Use, Trans Tech Publications LtdSwitzerland: 199–204.

You, D, Michelic, S K and Bernhard, C, 2020. Modeling of ladle refining process considering mixing and chemical reaction, *Steel Research International*, 91(11).

Zhang, H, Wu, M, Zhang, Z, Ludwig, A, Kharicha, A, Rónaföldi, A, Roósz, A, Veres, Z and Svéda, M, 2022. Experimental evaluation of MHD modeling of EMS during continuous casting, *Metallurgical and Materials Transactions B*, 53(4): 2166–2181.

Zhang, Y and Xu, Z, 2003. Kinetics of convective crystal dissolution and melting, with applications to methane hydrate dissolution and dissociation in seawater, *Earth and Planetary Science Letters*, 213(1-2): 133–148.